Outside Filament-wound Reinforcement: A Novel Configuration for FRP Bridge Decks

Peng Feng, Leiping Ye, Tianhong Li, Qianli Ma

Key Laboratory of Structural Engineering and Vibration of China Education Ministry
Department of Civil Engineering, Tsinghua University
Beijing, 100084, P.R. China

ABSTRACT: A novel configuration for FRP (fiber reinforced polymer) bridge decks, fiber filaments winding around it, is proposed. Three different types of FRP decks treated with this configuration and without it were tested and compared. The tests show that the OFR (outside filament-wound reinforcement) enhances the loading capacity of the decks by shifting their failure modes. An FRP deck product, HD, is developed based on the OFR procedure. The reinforcing mechanism of OFR is investigated by analyzing the test results and simulating the failure process with finite element software, which verifies the reinforcing effect of OFR.
KEYWORDS: FRP (fiber reinforced polymer) composite, bridge deck, corrosion resistance, light-weight superstructure, debonding, failure simulation.

1. INTRODUCTION

FRP(fiber reinforced polymer) bridge decks are increasingly used in existing bridges to replace the deteriorated decks or act as elements in new bridges which benefit from their favourable properties, such as corrosion resistance, convenient installation, light weight, good fatigue performance, and low maintenance cost. FRP decks adapt to the corrosion environments of deicing salt, sea water, and salina, which have only 20~40% self-weight of the conventional concrete or steel decks and more rapid construction process. As a result, FRP decks have been installed on more than 100 bridges in the past decade, mostly in America (Feng and Ye, 2004). The research on FRP bridge structures started in the 1970's initially aiming to build large span bridges. The first FRP highway bridge was built in Beijing, China in 1982 (Feng and Ye, 2004). The demand for FRP decks boomed as its advantages for common bridges became apparent after an FRP deck bridge was built over No-Name Creek, Russell, Kansas, in 1996 (Kansas Structural Composites Inc.,1997). Many FRP bridge deck products have been developed and studied (Feng and Ye, 2004). It was found from their failure modes in tests that the FRP longitudinal strength, which is much higher than the strengths in shear, transverse and inter-layer, wasn't efficiently utilized in most cases. And the brittle failure, which is indisposed for structures, always occurred (Feng et al, 2004). So it becomes a consequent issue for FRP decks to enhance ultimate loading capacity by utilizing the FRP longitudinal strength and improve their failure process characteristic. The safety factor is controlled by its strength although the stiffness sometimes is the major control parameter for design. To this end, OFR (outside filament-wound reinforcement), a novel configuration for FRP bridge decks, is presented. Three different types of FRP decks treated with OFR and without it are tested and compared, one of which is developed into a product, HD. The reinforcing mechanism of OFR is investigated to verify its effects based on finite element analysis and tests of HD decks.

2. PRE-INVESTIGATION OF EXISTING FRP DECKS

2.1 Types of FRP Deck

The existing FRP decks can be classified into four types according to their configurations, as listed in Table 1. The composite manufacturing processes, including layup, VARTM (vacuum aided resin transfer molding), pultrusion and filament winding, are employed to make these modular products. Even several processes are used for one product. The behaviors of FRP deck are correlated with the method of fabrication and assembly.

Table 1 Classification of FRP decks

Configuration	Fabrication/assembly		Representative literatures/cases
Sandwich deck	Hand/automated lay-up		No-name Creek Bridge(USA)
	RTM/VARTM		Bentley's Bridge(USA)
AMP (assembled modular profiles) deck	Coupled		Rama VIII Bridge Enclosure(Thailand)
	Bolted		Deck system of Zetterberg et al (2001)
	Bonded		Wickwire Run Bridge(USA)
	Prestressed		Deck system of Wu (2003)
	Combined above		Deck system of Sotiropoulos (1995)
CSC (combining skin-plates and core-profiles) deck	Tubes	Pultruded	Deck system of Brown and Zureick (2001)
		Filament wound	Deck system of Williams et al (2003)
	Face plates	Pultruded	Deck system of Temeles (2001)
		Layup	Deck system of Brown and Zureick (2001)
FRP-concrete/glulam hybrid deck			Toowoomba Bridge (USA)

2.2 Failure Modes

In tests of existing FRP bridge decks, the apparent failure characteristics--cracking, fiber breaking, debonding and delaminating--were observed as the loading capacity fell. Each failure mode has a corresponding loading capacity value. The damage always starts at the lowest mode, which leads to the failure of the whole deck. Therefore, it is reasonable to believe that deck performance can be improved by preventing these failure modes. According to the failing origin, the failure modes can be classified into strength failure, connection failure, and buckling. (i) Strength failure is the failure caused by the stress of FRP reaching the strength of material, including tensile, compressive, in-plane shear, bending, and inter-layer. The tensile and compressive failure in the weak direction, in-plane shear failure, bending failure, and inter-layer failure are frequent. An inter-layer strength failure example is shown in Figure 1(a). (ii) Connection failure is caused by the connection break FRP components, including bebonding, bolt shear, and bolt bearing. The adhesive bond is always employed for the existing FRP deck, so the debonding often occurs, as shown in Figure 1(b). This mode is undesirable because the FRP isn't utilized fully and breaks suddenly. (iii) Buckling failure is caused by the instability of the compressed FRP elements. The obvious buckling waves can be seen before the FRP elements fail in this mode as illustrated in Figure 1(c). As FRP is linear elastic, the FRP elements usually don't reach the maximum loading capacity when the local buckling occurs. In most cases, buckling failure goes together with the other two failure modes. This can occur in two ways: buckling failure precedes the other two, and buckling occurs after the other two. The former is the buckling failure strictly. All three failure modes may occur sequentially in the tests, even influence other each. But the key failure, which causes the loading capacity falling, is what concerns us. Usually, tensile and compressive failure in the weak direction, delaminating, in-plane shear failure, and debonding between components acted as the key modes in the tests of the existing FRP decks. Therefore, it is a way for improving the performance of FRP decks to prevent or defer these failure modes by configuration design, which is the main reason for the use of OFR.

(a) Strength failure: inter-layer (b) Connection faliure: debonding (c) Buckling

Figure 1 Failure modes of FRP decks

3. OFR FOR FRP DECKS

3.1 OFR Manufacture Procedure

The OFR configuration was invented for enhancing the loading capacity of FRP decks. The fiber filaments, which are dipped in resin, are wound around the whole FRP deck as the core in the cross-angle $\pm\theta$, as shown in Figure 2.The filaments are tensioned before being wound around the FRP deck so as to encase it. The performance of FRP decks which are confined by OFR is greatly improved. The failure modes corresponding with the lower loading capacities, in which FRP decks have a tendency to disperse and swell, including transverse cracking, bubbling, and debonding, all of which can be significantly constrained by OFRP treatment. Three different types of FRP decks were studied after OFR treatment as listed in Table 2.

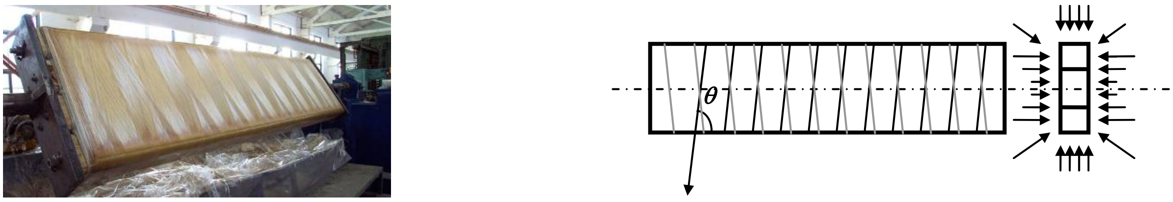

(a) Manufacture scene (b) Winding scheme

Figure 2 OFR manufacture procedure

3.2 FRP Decks with OFR: SPW, FDW and HDW

SP is a GFRP modular pultruded profile deck for footbridges. It is formed with E-glass roving (4800 Tex), continuous strand mat, and unsaturated polyester resin. An SP deck was wound with the filament around its cross section, which is called SPW. The E-glass roving (1200 Tex) and epoxy resin compose the filament wound layer 2.2mm thick. The winding angle is ±80° and the fiber volume fraction is 0.55. The CSC deck for highway bridges, named FD deck is the first generation product. It is combined with pultruded GFRP profiles and lay-up face plates. The pultrusions are composed of E-glass rovings (2400 Tex), continuous strand mat and unsaturated polyester resin. The plates are laid up with E-glass strand mat and unsaturated polyester resin. Epoxy resin bonds them together. An FD deck was treated with the same OFR layer as SPW, named FDW. The second generation CSC FRP deck product for highway bridges was named HD deck. HD deck is composed of two pultruded GFRP face plates and four filament-wound square tubes bonded with epoxy adhesive. The plates, which are 12mm thick altogether, are composed of roving layers, fabric layers, and mat layers. The tubes are made of E-glass and epoxy resin. Their average wall thickness is 8mm. The gaps and the filleted corner are filled with resin mortar. Two HD decks are treated with different thickness OFR: 3mm and 5mm, which are named HDW3 and HDW5 respectively.

Table 2 Specimens in Test Program

Configuration of decks	Specimens	OFR	Span(m)	Loading conditions
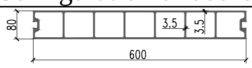	SP	None	1.3	Central line (10mm width)
	SPW	2.2mm, ±80°	1.3	
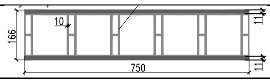	FD	None	1.3	Central point (200×200mm)
	FDW	2.2mm, ±80°	1.3	
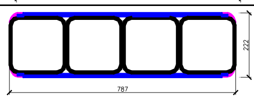	HD0	None	2.8	Case 1: 4-point line bending Case 2: central point (200×200mm)
	HDW3	3.0mm, ±80°	2.8	
	HDW5	5.0mm, ±80°	2.8	

4. EXPERIMENTAL RESEARCH

Seven specimens, three groups of FRP decks, were tested and compared as listed in Table 2. All decks are simple supported. There are three kinds of loading conditions, of which the central point simulates the wheel load.

4.1 SP vs. SPW

The load was applied on SP and SPW gradually to avoid sudden collapse. Some clacks began to appear for SP when the load reached 30kN, while it was at 40kN for SPW. It was noticed however that there was no sound emitted when the load reached the same level in the second loading after unloading from the evaluated maximum load. It can be concluded that the clacks are the signal of damage developing. With continuous increase in load, denser clacks were heard. SP reached its ultimate load by sounding loudly during failure, a crack along the top edge of the section occurred on one side, and the top plate delaminated and buckled as shown in Figure 1(a). The thickness of the delaminated layer was about 3mm and the crack length was about 480 mm. Moreover, there was a crack on the other edge of the decks. For SPW, it had exhibited similar behavior as loading increased except that the ultimate load was much higher than SP and resulted in a different failure mode. At the ultimate failure point, a longitudinal crack appeared on each inner web. The cracks extended from the span center to one support end in one half of the span only. Under the distributing beam at the center loading position, there was a vertical crack on the outside wound layer. Both SP and SPW displayed linear behavior throughout the loading history, as illustrated in Figure 3. Compared with SP, the failure mode has been changed; the ultimate load of SPW increased 59% with 12.7% increase in stiffness.

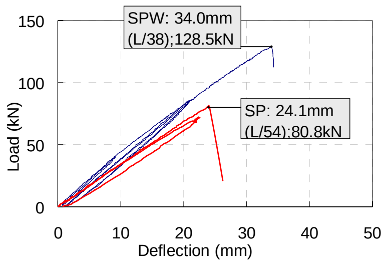

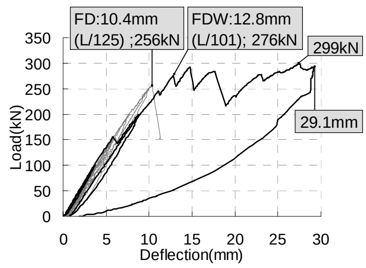

Figure 3 Load-deflection relation of SP and SPW **Figure 4 Load-deflection curves for FD and FDW**

4.2 FD vs. FDW

FD and FDW, which were loaded at the center of decks, are bent in two directions. With the load increasing, the phenomena of the clacks were similar to that with SP and SPW. For FD, the first clack load was 50kN and the behavior was linear until the ultimate load 256kN. However, the behavior of FDW has different as the pseudo-ductility appeared. Their load-deflection curves are shown in Figure 4. On the curve of FDW, the point at 276kN and 12.8mm can be defined as the nominal yield point, the ultimate deflection is 29.1mm and the maximum load is 299kN. The ductile behavior was not provided by the plastic deformation of material because FRP is a linear elastic material, but actually by fraction and sliding of the interface between the components. The deflection of FDW is recoverable with unloading as shown in Figure 4. FD's failure mode was debonding between the assembled profiles and the bottom plate as shown in Figure 1(b); FDW's failure mode was changed, due to OFR, which effectively confined the assembled profiles and the plates. The ultimate failure was caused by the cracks on the two webs under the loading patch. The load patch obviously was sunken. And there was a slippage between the profiles and the bottom plate. Compared with FD, the maximum load of FDW increased 16.8% with a little increase in stiffness. It is the most significant effect that the deformability of FDW was more than doubled and had a yieldable characteristic.

4.3 HD0, HDW3 and HDW5

HD group was loaded in two cases: 4-piont line bending to estimate the stiffness and central point loading to simulate the wheel load. HD0 and HDW3 loaded to failure under Case 2. For HD0, the debonding between tubes and bottom plate occurred suddenly when the central load reached 485kN as shown in Figure 5. Before it, HD0 was linear elastic almost. HDW3 had a little ductile failure process by the punching failure under the load position as shown in Figure 6. It started from the load of 590kN. The maximum load reached 618kN. Comparing HDW3 and HD0, the load capacity had a 26.4% increase. HDW5 didn't fail when the load went over the maximum value of the other two in Case 2.Their load-deflection curves are compared in Figure 7. HDW5 was loaded to failure at 1737kN in Case 1. Before failure, the deck deformed obviously as shown in Figure 8(a). The deck was broken in bending, and the tubes were crushed as shown in Figure 8(b) and (c). In this mode, FRP is utilized effectively although it failed brittle. Comparing three decks, the ultimate strength increase with the thickness of the OFR layer is shown.

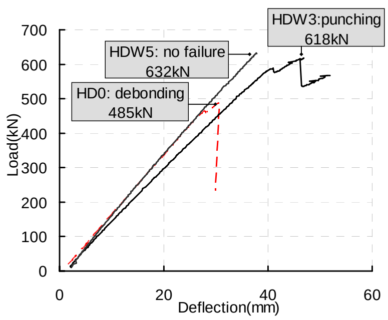

Figure 5 Debonding of HD0 **Figure 6 Punching of HDW3** **Figure7 Load-deflection curves in Case 2**

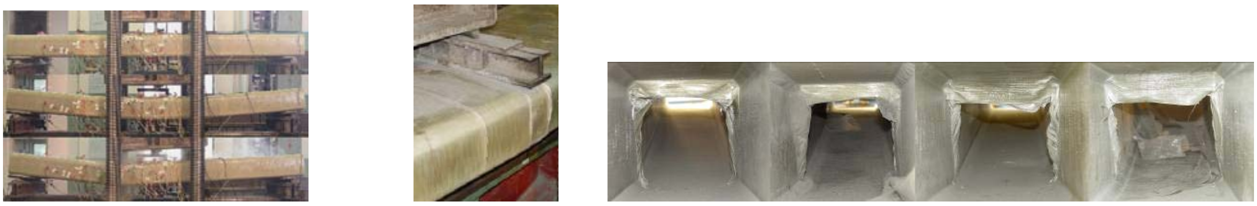

(a) No load, before failure and failing (b) Crack of OFR (c) Crushing of core tubes

Figure 8 Failure of HDW5

From these tests, the effects of OFR were proved to enhance the ultimate load capacity and slowed down or curtailed the failure process. To expose the roles of OFR in this enhancement, a mechanics analysis was conducted.

5 MECHANICSM ANALYSIS

5.1 Failure Process Simulation

As the debonding failure between core and face plate in test was avoided by the use of OFR, its most considerable effect, this failure mode was simulated with finite element software ANSYS. The pre-crack method was used. There had been a rectangle crack between core and bottom plate in the FEA model before loading. The depth of the crack was defined as *c*, the width of crack was 2*c*. It expends from one side to the other while *c* increases step by step under a certain load. Figure 9 shows the failure process in Case 2. The stiffness and the deformation are investigated at each step. The deflection of the center is noted as *Y*. The increment of *Y* over the increment of *c* in each step, $\Delta Y/\Delta c$, shows the development of the crack. When it goes down with the crack increasing, the crack develops unstably, and the debonding occurs. Figure 12 shows the relationship of the HD deck with different OFR layer thicknesses, t_r. It can be seen that t_r=0, no OFR, debonds; t_r=1mm is closed to the critical state. The critical thickness $t_{r,c}$ can be determined by equivalent stiffness, as follows,

$$t_{r,c} = \frac{BG_{yz}}{2G_a} \tag{1}$$

where G_{yz} is in-plane shear stiffness of OFR, G_a is the shear stiffness of the adhesive layer between core and plate, *B* is the width of bonded area.

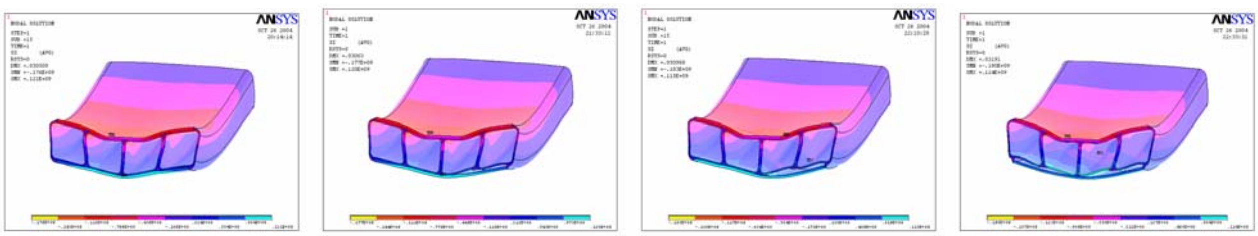

(a) *c*=0.1 (b) *c*=0.3 (c) *c*=0.5 (d) *c*=0.71(width of deck)

Figure 9 Debonding failure simulation of HDW

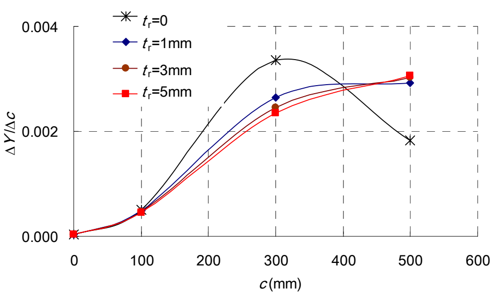

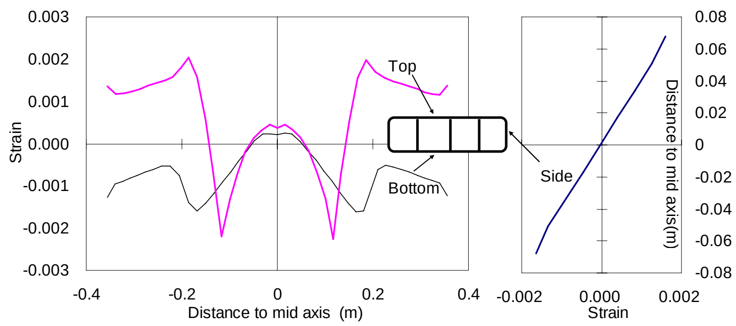

Figure 10 Crack developing trend and depth

Figure 11 Longitudinal strain distribution of OFR

5.2 Strains in OFR

Finite element analysis is used for simulating the behavior of the HD deck. The ideal bonds are considered under lower load. In Case 2, the OFR strain in transverse can be picked up as shown in Figure 11. It can be seen that there are peak strains at the corners, the edge of the loading patch, and the joint of face and rib in the trend of the top in tension except the loading part and the bottom in compression mainly. In the FEA of pre-cracked HDW, there is an obviously high shear stress area near the crack as shown in Figure 12. The plate and the core can work together with the OFR layer to transfer the shear force. From the strain distribution of OFR, it is concluded that there are two actions mainly: bearing the shear force released from the crack and enhancing the local properties in transverse.

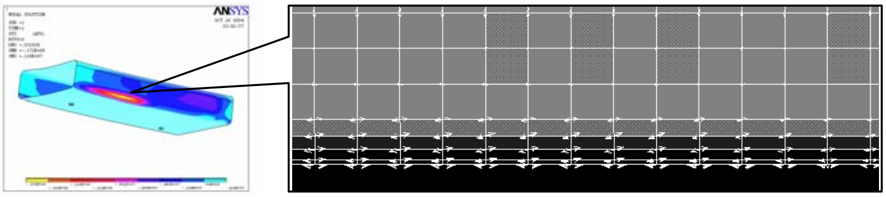

Figure 12 Shear stress distribution of OFR in Pre-cracked HDW

6 CONCLUSIONS

The outside filament-wound reinforcement is presented. Three different configurations of decks were tested. The mechanics was studied by tests and FEA. The conclusions are summarized as below.

(1) OFR is an effective configuration for improvement of FRP decks behavior in the loading capacity and the failure ductility.

(2) The failure mode shifting is the exhibition of OFR effect mechanics as the failure mode corresponding with lower loading capacity is avoided.

(3) OFR layers bear the shear force released from the crack and strengthen the local area in transverse in the FRP decks.

ACKNOWLEDGEMENTS

The authors are grateful to the Natural Science Foundation of China for their support to the research presented here through a national key project on the application of FRP composites in civil engineering in China (No. 50238030).

REFERENCES

Brown R.T., and Zureick A.H. (2001). Lightweight composite truss section decking. *Marine Structures*, 14, 115-132.

Feng P., and Ye L.P. (2004). Applications and research on fiber reinforced polymer bridge decks. *Industrial Construction*, 34:370, 290-301 (in Chinese).

Feng P., Ye L.P., and Zhang L.W., et al.(2004). Experimental study of outside filament winding reinforced FRP bridge decks. *Proceeding of 4th International Conference on Advanced Composite Materials in Bridges and Structures (ACMBS-4)*, Calgary, Alberta, Canada, (CD-ROM).

Kansas Structural Composites Inc. (1997). Fiber-reinforced polymer honeycomb short span bridge for rapid installation. *IDEA Project Final Report*, Web site: *http://www.ksci.com*.

Sotiropoulos S.N. (1995). Performance of FRP components and connections for bridge deck systems. *PhD Dissertation*, West Virginia Univ., Morgantown, USA.

Temeles A.B. (2001). Field and laboratory tests of a proposed bridge deck panel fabricated from pultruded fiber-reinforced polymer components. *M.S. Thesis*, Virginia Polytechnic Inst. and State Univ. Blacksburg, USA.

Williams B., Shehata E. and Rizkalla S.H. (2003). Filament-wound glass fiber reinforced polymer bridge deck modules. *Journal of Composites for Construction, ASCE*, 7, 266-273.

Wu Z.H.(2003). Prestressed FRP tubular deck system. *M.S. Thesis*, North Carolina State Univ., USA.

Zetterberg T., Astrom B.T., and Backlund, J. et al. (2001). On design of joints between composite profiles for bridge deck applications. *Composite Structures*, 51, 83-91.